

Complete plastome sequences from *Bertholletia excelsa* and 23 related species yield informative markers for Lecythidaceae

Ashley M. Thomson^{1,2*}, Oscar M. Vargas^{1*} , and Christopher W. Dick^{1,3} 

Manuscript received 1 October 2017; revision accepted 11 January 2018.

¹ Department of Ecology and Evolutionary Biology, University of Michigan, Ann Arbor, Michigan 48109, USA

² Faculty of Natural Resources Management, Lakehead University, Thunder Bay, Ontario P7B 5E1, Canada

³ Smithsonian Tropical Research Institute, Panama City 0843-03092, Republic of Panama

⁴ Author for correspondence: oscarvargash@gmail.com

*These authors contributed equally to this work.

Citation: Thomson, A. M., O. M. Vargas, and C. W. Dick. 2018. Complete plastome sequences from *Bertholletia excelsa* and 23 related species yield informative markers for Lecythidaceae. *Applications in Plant Sciences* 6(5): e1151.

doi:10.1002/aps3.1151

PREMISE OF THE STUDY: The tropical tree family Lecythidaceae has enormous ecological and economic importance in the Amazon basin. Lecythidaceae species can be difficult to identify without molecular data, however, and phylogenetic relationships within and among the most diverse genera are poorly resolved.

METHODS: To develop informative genetic markers for Lecythidaceae, we used genome skimming to de novo assemble the full plastome of the Brazil nut tree (*Bertholletia excelsa*) and 23 other Lecythidaceae species. Indices of nucleotide diversity and phylogenetic signal were used to identify regions suitable for genetic marker development.

RESULTS: The *B. excelsa* plastome contained 160,472 bp and was arranged in a quadripartite structure. Using the 24 plastome alignments, we developed primers for 10 coding and non-coding DNA regions containing exceptional nucleotide diversity and phylogenetic signal. We also developed 19 chloroplast simple sequence repeats for population-level studies.

DISCUSSION: The coding region *ycf1* and the spacer *rpl16-rps3* outperformed plastid DNA markers previously used for barcoding and phylogenetics. Used in a phylogenetic analysis, the matrix of 24 plastomes showed with 100% bootstrap support that *Lecythis* and *Eschweilera* are polyphyletic. The plastomes and primers presented in this study will facilitate a broad array of ecological and evolutionary studies in Lecythidaceae.

KEY WORDS Amazonian trees; *Bertholletia excelsa*; DNA barcoding; genetic markers; Lecythidaceae; plastome.

Lecythidaceae (sensu lato) is a pantropical family of trees with three subfamilies: Foetidioideae, which is restricted to Madagascar; Barringtonioideae, found in the tropical forests of Asia and Africa; and the Neotropical clade Lecythidoideae, which contains approximately 234 of the approximately 278 known species in the broader family (Mori et al., 2007, 2017; Huang et al., 2015; Mori, 2017). Neotropical Lecythidaceae are understory, canopy, or emergent trees with distinctive floral morphology and woody fruit capsules. Among Lecythidaceae species are the iconic Brazil nut tree, *Bertholletia excelsa* Bonpl.; the oldest documented angiosperm tree, *Cariniana micrantha* Ducke (dated at >1400 years old in Manaus, Brazil; Chambers et al., 1998); the cauliflorous cannonball tree commonly grown in botanical gardens, *Couroupita guianensis* Aubl.; and important timber species (e.g., *Cariniana legalis* (Mart.) Kuntze). Lecythidaceae is the third most abundant family of trees in the Amazon forest, following Fabaceae and Sapotaceae (ter Steege

et al., 2013). The most species-rich genus, *Eschweilera* Mart. ex DC., with approximately 99 species (Mori, 2017), is also the most abundant tree genus in the Amazon basin (ter Steege et al., 2013), and *E. coriacea* (DC.) S. A. Mori is the most common tree species in much of Amazonia (ter Steege et al., 2013). Lecythidaceae provide important ecological services such as carbon sequestration and are food resources for pollinators (bats and large bees) and seed dispersers (monkeys and agouties) (Prance and Mori, 1979; Mori and Prance, 1990).

Tools for species-level identification and phylogenetic analyses of Lecythidaceae could significantly advance research on Amazon tree diversity. However, despite their ease of identification at the family level, species-level identification of many Lecythidaceae (especially *Eschweilera*) is notoriously difficult when based on sterile (i.e., without fruit or floral material) herbarium specimens, and flowering of individual trees often occurs only at multi-year intervals (Mori and

Prance, 1987). As a complement to other approaches, DNA barcoding (Dick and Kress, 2009; Dexter et al., 2010) may help to identify species or clades of Lecythidaceae.

A combination of two protein-coding plastid regions (*matK* and *rbcL*) has been proposed as a core plant DNA barcode (Hollingsworth et al., 2009), although other coding and non-coding plastome regions (*psbA-trnH*, *rpoB*, *rpoC1*, *trnL*, and *ycf5*) and the ITS of nuclear ribosomal genes have been recommended

as supplemental barcodes for vascular plants (Kress et al., 2005; Lahaye et al., 2008; Li et al., 2011). However, an evaluation of a subset of these markers (ITS, *psbA-trnH*, *matK*, *rbcL*, *rpoB*, *rpoC1*, and *trnL*) on Lecythidaceae in French Guiana (Gonzalez et al., 2009) showed poor performance for species identification. Furthermore, the use of traditional markers (plastid *ndhF*, *trnL-F*, and *trnH-psbA*, and nuclear ITS) for phylogenetic analysis has produced weakly supported trees (Mori et al., 2007; Huang et al., 2015), indicating a

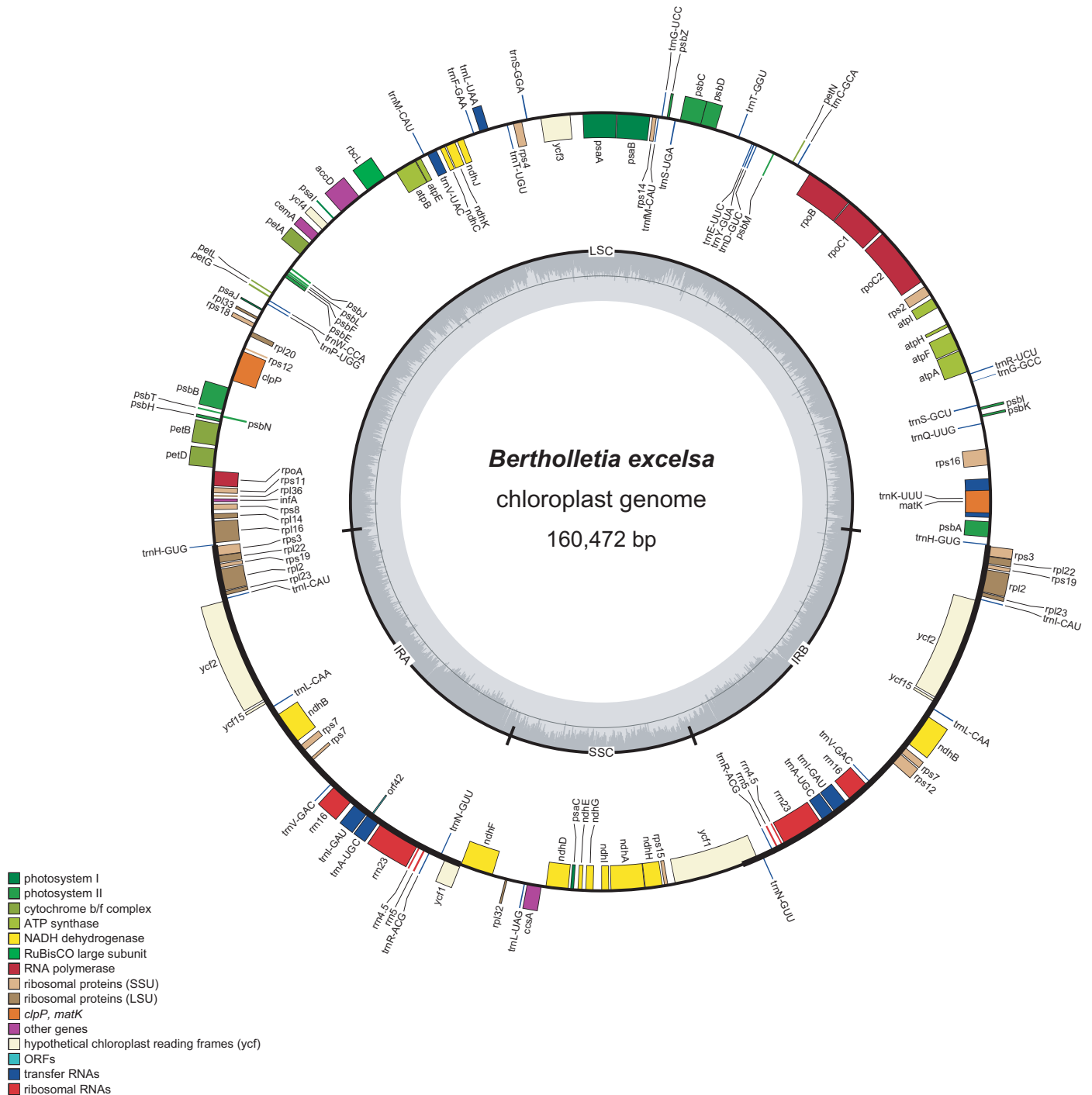


FIGURE 1. Plasmome map of the Brazil nut tree, *Bertholletia excelsa*. Genes outside of the circle are transcribed clockwise; genes inside of the circle are transcribed counterclockwise. Gray bars in the inner ring show the GC content percentage.

need to develop more informative markers and/or increase molecular sampling.

The main objectives of this study were to (1) assemble, annotate, and characterize the first complete plastome sequence of Lecythidaceae from the iconic Brazil nut tree, *B. excelsa*; (2) obtain a robust backbone phylogeny for the Neotropical clade using newly assembled draft plastome sequences for an additional 23 species; and (3) develop a novel set of informative molecular markers for DNA barcoding and broader evolutionary studies.

METHODS

Plant material and DNA library preparation

We performed genomic skimming on 24 Lecythidaceae species, including 23 Lecythidoideae and one outgroup species (*Barringtonia*

edulis Seem.) from the Barringtonioideae. The sampling included all 10 Lecythidoideae genera (Appendix 1). Silica-dried leaf tissue from herbarium-vouchered collections was collected by Scott Mori and colleagues and loaned by the New York Botanical Garden. Total genomic DNA was extracted from 20 mg of dried leaf tissue using the NucleoSpin Plant II extraction kit (Machery-Nagel, Bethlehem, Pennsylvania, USA) with SDS lysis buffer. Prior to DNA library preparation, 5 µg of total DNA was fragmented using a Covaris S-series sonicator (Covaris Inc., Woburn, Massachusetts, USA) following the manufacturer's protocol to obtain approximately 300-bp insert sizes. We prepared the sequencing library using the NEBNext DNA library Prep Master Mix and Multiplex Oligos for Illumina Sets (New England BioLabs Inc., Ipswich, Massachusetts, USA) according to the manufacturer's protocol. Size selection was carried out prior to PCR using Pippin Prep (Sage Science, Beverly, Massachusetts, USA). Molecular mass of the finished paired-end library was quantified using an Agilent 2100 Bioanalyzer (Agilent

TABLE 1. Genes contained within the chloroplast genome of *Bertholletia excelsa*.

Function	Gene group	Gene name
Self-replication	Ribosomal proteins (large subunit)	<i>rpl2, rpl14, rpl16, rpl20, rpl22, rpl23, rpl32, rpl33, rpl36</i>
	Ribosomal proteins (small subunit)	<i>rps2, rps3, rps4, rps7, rps8, rps11, rps12, rps14, rps15, rps16, rps18, rps19</i>
	RNA polymerase subunits	<i>rpoA, rpoB, rpoC1, rpoC2</i>
	Ribosomal RNAs	<i>rrn4.5, rrn5, rrn16, rrn23</i>
	Transfer RNAs	<i>trnA-UGC, trnC-GCA, trnD-GUC, trnE-UUC, trnF-GAA, trnG-GCC, trnG-UCC, trnH-GUG, trnI-CAU, trnI-GAU, trnK-UUU, trnL-CAA, trnL-UAA, trnL-UAG, trnM-CAU, trnM-CAU, trnN-GUU, trnP-UGG, trnQ-UUG, trnR-AGC, trnR-UCU, trnS-GCU, trnS-GGA, trnS-UGA, trnT-GGU, trnT-UGU, trnV-GAC, trnV-UAC, trnW-CCA, trnY-GUA</i>
Photosynthesis	Photosystem I	<i>psaA, psaB, psaC, psal, psaJ</i>
	Photosystem II	<i>psbA, psbB, psbC, psbD, psbE, psbF, psbH, psbI, psbJ, psbK, psbL, psbM, psbN, psbT, psbZ</i>
	NADH dehydrogenase	<i>ndhA, ndhB, ndhC, ndhD, ndhE, ndF, ndhG, ndhH, ndhI, ndhJ, ndhK</i>
	Cytochrome b/f complex	<i>petA, petB, petD, petG, petL, petN</i>
	ATP synthase	<i>atpA, atpB, atpE, atpF, atpH, atpI</i>
Other genes	RuBisCO large subunit	<i>rbcl</i>
	Subunit of acetyl-CoA-carboxylase	<i>accD</i>
	Envelope membrane protein	<i>cemA</i>
	Protease	<i>clpP</i>
	c-type cytochrome synthase	<i>ccsA</i>
	Translational initiation factor	<i>infA</i>
Unknown function	Maturase	<i>matK</i>
	Hypothetical chloroplast reading frames	<i>ycf1, ycf2, ycf3, ycf4, yc15</i>

TABLE 2. Comparison for plastome subunits for the samples for which the inverted repeats were completely assembled.^a

Species	LSC length (bp)	SSC length (bp)	IR length (bp)	GC content (%)	Protein-coding genes	rRNAs	tRNAs
<i>Allantoma decandra</i>	85,269	18,738	27,618	36.9	81	4	30
<i>A. lineata</i>	85,119	18,756	27,635	36.9	81	4	30
<i>Bertholletia excelsa</i>	85,840	18,950	27,841	36.4	81	4	30
<i>Corythophora amapaensis</i>	85,861	18,778	27,638	36.7	81	4	30
<i>C. labriculata</i>	85,673	18,759	27,594	36.7	81	4	30
<i>Couratari macrosperma</i>	83,785	18,728	27,614	37.0	81	4	30
<i>C. stellata</i>	85,547	18,491	27,576	36.9	81	4	30
<i>Eschweilera alata</i>	85,056	18,721	27,635	36.6	81	4	30
<i>E. caudiculata</i>	84,713	18,759	27,638	37.0	81	4	30
<i>E. congestiflora</i>	84,815	18,167	27,715	37.1	81	4	30
<i>E. integrifolia</i>	84,688	18,796	27,592	36.9	81	4	30
<i>E. micrantha</i>	85,286	18,719	27,668	36.8	81	4	30
<i>E. wachenheimii</i>	85,378	18,815	27,603	36.8	81	4	30
<i>Lecythis pneumatophora</i>	85,506	18,845	27,622	36.7	81	4	30

Note: IR = inverted repeat; LSC = large single-copy region; SSC = small single-copy region.

^aLength and GC content of the large single-copy and small single-copy regions in partial plastomes are estimates only.

TABLE 3. Primers for the amplification of simple sequence repeats in the plastome of *Bertholletia excelsa*. All primer pairs amplify non-coding sequences with the exception of *ndhD*.^a

Forward primer sequence (5'–3')	Reverse primer sequence (5'–3')	Repeat unit	Location	Region	No. of repeats	Product size (bp)
CCAAAATCATGAACTAACCCCA	ACCAAGAGGGCGTTATTGCT	A	396–409	<i>trnH-psbA</i>	14	226
TGAAGTCGTGTGTGATGATCT	CTGTTGATAAGTTTCCGAGGT	C	3686–3702	<i>trnK intron</i>	17	197
GAGGTTTTCTCCTCGGACGG	ACCACTCATTAAACGAAATGCCT	A	5680–5691	<i>rps16 intron</i>	12	244
GTCCACTCAGCCATCTCTCC	AGCCCGGCCATAGGAATAAA	AAAG	9396–9407	<i>trnS-trnG</i>	3	297
TTTATTCTATGCGCGGGCT	TGCATTGTTAAGAAATCCATGTTTCA	A	9769–9780	<i>trnS-trnG</i>	12	246
TTTTCCCCACACTTCCCCTC	TGTCGGTCATTGATTGTTG	A	17,925–17,938	<i>rps2-rpoC2</i>	14	192
AAGAGAGGAGAAGTTTTAGGCA	CCTTACCACTCGGCCATGTC	A	29,392–29,403	<i>rpoB-trnC</i>	12	232
GGGATGCGAGAAAGAGACTT	CAAAAGTATATCTTTCTACGGGTCG	AAAG	34,775–34,786	<i>trnT-psbD</i>	3	250
TACCGGTTTTCAAGACCGGG	TCACAAATGGGCATGCTGGA	AAAAT	38,160–38,174	<i>trnS-psbZ</i>	3	201
ACCCATCAATCATTGATTCGT	GAAAGATCTTTCCTTGGGGGA	AAAG	47,627–47,638	<i>ycf3-trnS</i>	3	168
No suitable primers found	No suitable primers found	AAAT	49,610–49,625	<i>trnT-trnL</i>	4	NA
No suitable primers found	No suitable primers found	AATT	50,016–50,027	<i>trnT-trnL</i>	3	NA
CCAATGAACAAGGGAGAGCC	ACCAAGGCAAACCCATGGAA	AAAATT	75,475–75,492	<i>clpP-psbB</i>	3	128
TGAATCACTGCTTTTCTTTGACTCT	AGGCGGTTCTCGAAAGAAGA	AAAAT	77,155–77,169	<i>psbB-psbT</i>	3	183
TTCAATCTCGGGATCTTTGAGA	TCGCCTGCGAAAACCTAACT	A	85,073–85,085	<i>rpl16-trnH</i>	13	246
TCGATCAATCCCTTTGCCT	CGTACTCCTCGCTCAATGAGA	AAAT	102,172–102,183	<i>rps12-trnV</i>	3	248
TGGAGCACCTAACACGCAT	AGACCTCCGGGAAAAGCATG	A	106,208–106,219	<i>trnL intron</i>	12	119
AGAGTAAACACAAGATACAAGGGT	GTGGTTAGGTCAATCGGGA	AACTT	117,345–117,359	<i>rpl32-trnL</i>	3	194
AGTCAACGTCAAAATTAATGAATGGT	AGGTTGAACGCGAGCGATAT	AT	117,609–117,622	<i>rpl32-trnL</i>	7	177
AAATAACTCCCGCGGTCCAG	GCTTCTTTGCATTACCGGG	AAAT	119,729–119,740	<i>ndhD</i>	3	240
No suitable primers found	No suitable primers found	AAT	122,820–122,831	<i>ndhG-ndhI</i>	4	NA
No suitable primers found	No suitable primers found	AAT	122,843–122,854	<i>ndhG-ndhI</i>	4	NA
AACCCGCTTCAAGCCATGAT	AAACGGCTTATAAATTCGCATG	AATC	125,271–125,282	<i>ndhA intron</i>	3	130

Note: NA = not applicable.

^aSequences have been deposited to GenBank (BioProject SUB2740669).

Technologies Inc., Santa Clara, California, USA) and by quantitative PCR using an ABI PRISM 7900HT (Thermo Fisher Scientific, Waltham, Massachusetts, USA) at the University of Michigan DNA Sequencing Core (Ann Arbor, Michigan, USA). We sequenced the libraries on one lane of the Illumina HiSeq 2000 (Illumina Inc., San Diego, California, USA) with a paired-read length of 100 bp.

Plastome assembly—Illumina adapters and barcodes were excised from raw reads using Cutadapt version 1.4.2 (Martin, 2011). Reads were then quality filtered using Prinseq version 0.20.4 (Schmieder and Edwards, 2011), which trimmed 5' and 3' sequence ends with a Phred quality score <20 and removed all trimmed sequences <50 bp in length, with >5% ambiguous bases, or with a mean Phred quality score <20. A combination of de novo and reference-guided approaches was used to assemble the plastomes. First, chloroplast reads were separated from the raw read pool by BLAST-searching all raw reads against a database consisting of all complete angiosperm plastome sequences available on GenBank (accessed in 2014). Any aligned reads with an *E*-value <1⁻⁵ were retained for subsequent analysis. The filtered chloroplast reads were de novo assembled using Velvet version 7.0.4 (Zerbino and Birney, 2008) with *k*-mer values of 71, 81, and 91 using a low-coverage cutoff of 5 and a minimum contig length of 300. The assembled contigs were then mapped to a reference genome (see below) using Geneious version R8 (Kearse et al., 2012) to determine their order and direction using the reference-guided assembly tool with medium sensitivity and iterative fine-tuning options. Finally, raw reads were iteratively mapped onto the draft genome assembly to extend contigs and fill gaps using the low-sensitivity, reference-guided assembly in Geneious. We first assembled the draft genome of *B. excelsa*; the plastomes of the remaining 23 species were assembled

subsequently using the plastome of *B. excelsa* as a reference. The *B. excelsa* plastome was annotated using DOGMA (Wyman et al., 2004) with the default settings for chloroplast genomes. Codon start and stop positions were determined using the open reading frame finder in Geneious and by comparison with the plastome sequence of *Camellia sinensis* (L.) Kuntze var. *pubilimba* Hung T. Chang (GenBank ID: KJ806280). A circular representation of the *B. excelsa* plastome was made using OGDRAW V1.2 (Lohse et al., 2007). The complete annotated plastome of *B. excelsa* and the draft plastomes of the remaining 23 Lecythidaceae species sampled were deposited into GenBank (Appendix 1).

Identification of molecular markers—Chloroplast simple sequence repeats (cpSSRs) in *B. excelsa* were identified using the Phobos Tandem Repeat Finder version 3.3.12 (Mayer, 2010) by searching for uninterrupted repeats of nucleotide units of 1 to 6 bp in length, with thresholds of ≥12 mononucleotide, ≥6 dinucleotide, and ≥4 trinucleotide repeats, and ≥3 tetra-, penta-, and hexanucleotide repeats (Sablok et al., 2015). We developed primers to amplify the cpSSRs using Primer3 version 2.3.4 (Untergasser et al., 2012) with the default options and setting the PCR product size range between 100 and 300 bp.

The 24 plastomes were aligned with MAFFT version 7.017 (Katoh et al., 2002) and then scanned for regions of high nucleotide diversity (π ; Nei, 1987) using a sliding window analysis implemented in DNAsp version 5.10.1 (Librado and Rozas, 2009) with a window and a step size of 600 bp. Levels of nucleotide diversity were plotted using the native R function “plot” (R Core Team, 2017), and windows with values over the 95th percentile were considered of high π .

Taking into account that DNA barcodes can also be used in phylogenetic analyses and because regions with high π do not

necessarily have high phylogenetic signal (e.g., unalignable hypervariable regions), we employed a log-likelihood approach modified from Walker et al. (2017) to identify phylogenetically influential regions. First, we inferred a phylogenetic tree with the plastome alignment (including only one inverted repeat) by performing 100 independent maximum likelihood (ML) searches using a GTRGAMMA model with RAxML version 8.2.9 (Stamatakis, 2014). Those searches resulted in the same topology that was subsequently annotated with the summary from 100 bootstraps using “sumtrees.py” version 4.10 (Sukumaran and Holder, 2010). We then calculated site-specific log-likelihoods in the alignment over the plastome phylogeny and calculated their differences site-wise to the averaged log-likelihood per site of 1000 randomly permuted trees (tips were randomly shuffled). Log-likelihood scores were calculated with RAxML using a GTRGAMMA model. The site-wise log-likelihood differences (LD) were calculated using 600-bp non-overlapping windows with a custom R script (see below). We interpreted greater LD as an indication of greater phylogenetic signal, and windows with an LD above the 95th percentile were considered to have exceptional phylogenetic signal.

Primers flanking the top 10 regions with high π were designed using Primer3 with default program options. We employed a maximum product size of 1300 bp because lower cutoff values (i.e., 600 bp) made the primer design extremely challenging due to

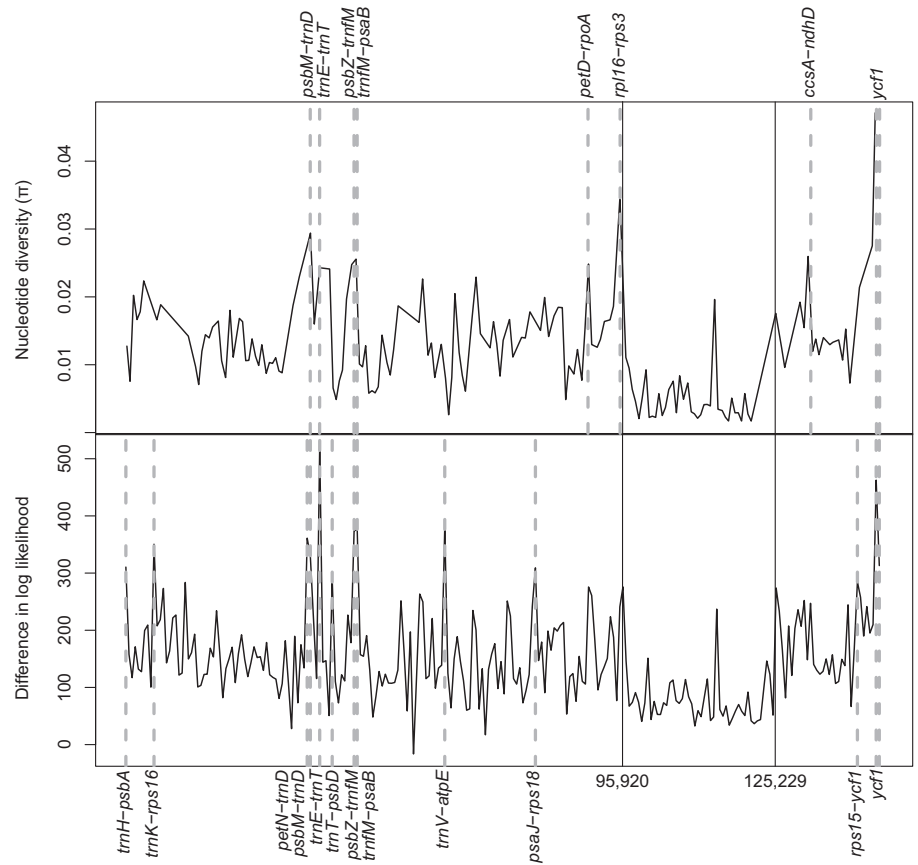


FIGURE 2. Sliding 600-site window analyses on the Lecythidaceae plastome alignment of 24 species showing nucleotide diversity (π) (top) and alignment site-wise differences in log-likelihood (LD) calculated from the chloroplast topology versus the average scores of 1000 random trees (bottom). Regions with π and LD above the 95th percentiles are indicated with dashed lines. Continuous vertical lines indicate the boundaries, from left to right, among the large single copy, the inverted repeat, and the small single copy.

TABLE 4. Regions of the plastome alignment (windows of 600 sites) with significantly high (above the 95th percentile) nucleotide diversity and/or site-wise log-likelihood score differences.^a

Location in the alignment	<i>Bertholletia</i> plastome location	Closest flanking expressed region		Region	π	LD
		5'	3'			
1–600	1–490	<i>trnH</i>	<i>psbA</i>	LSC		*
5401–6000	4885–5373	<i>trnK-UUU</i>	<i>rps16</i>	LSC		*
34,801–35,400	30,925–31,450	<i>petN</i>	<i>trnD-GUC</i>	LSC		*
35,401–36,000	31,451–31,967	<i>psbM</i>	<i>trnD-GUC</i>	LSC	*	*
37,201–37,800	33,027–33,573	<i>trnE-UUC</i>	<i>trnT-GGU</i>	LSC	*	*
39,601–40,200	34,893–35,433	<i>trnT-GGU</i>	<i>psbD</i>	LSC		*
43,801–44,400	38,798–39,254	<i>psbZ</i>	<i>trnM-CAU</i>	LSC	*	*
44,401–45,000	39,255–39,744	<i>trnM-CAU</i>	<i>psaB</i>	LSC	*	*
61,201–61,800	54,771–55,275	<i>trnV-UAC</i>	<i>atpE</i>	LSC		*
78,601–79,200	70,230–70,771	<i>psaJ</i>	<i>rps18</i>	LSC		*
89,401–90,000	80,536–81,103	<i>petD</i>	<i>rpoA</i>	LSC	*	
95,401–96,000	85,455–85,906	<i>rpl16</i>	<i>rps3</i>	LSC	*	
131,401–132,000	119,237–119,759	<i>ccsA</i>	<i>ndhD</i>	SSC	*	
140,401–141,000	127,827–128,402	<i>rps15</i>	<i>ycf1</i>	SSC		*
144,001–144,600	131,283–131,868	<i>ycf1</i>	<i>ycf1</i>	SSC	*	*
144,601–145,200	131,869–132,446	<i>ycf1</i>	<i>ycf1</i>	SSC	*	*

Note: π = nucleotide diversity (see main text); LD = log-likelihood score differences; LSC = large single copy; SSC = small single copy.

^aSignifies regions with high (above the 95th percentile) nucleotide diversity or site-wise log-likelihood score differences.

^bCoding regions are indicated in windows that have the same 5' and 3'-expressed flanking regions in column 3. Notice that no regions are reported for the inverted repeat (IR). Coordinates are given on the alignment and the *Bertholletia excelsa* plastome that are assembled with the standard LSC-SSC-IR structure.

TABLE 5. Nucleotide diversity and differences in log-likelihood scores of the informative windows identified in this study and of previously proposed barcode markers.

Region ^a	π^b	LD ^b
<i>ccsA-ndhD</i>	0.0258	247.12
<i>matK</i>	0.0153	136.92
<i>petD-rpoA</i>	0.0246	260.79
<i>petN-trnD</i>	0.0228	361.07
<i>psaJ-rps18</i>	0.0176	309.10
<i>psbM-trnD</i>	0.0292	330.41
<i>psbZ-trnfM</i>	0.0246	373.97
<i>rbcl</i>	0.0105	95.03
<i>rpl16-rps3</i>	0.0345	275.89
<i>rpoB</i>	0.0097	120.53
<i>rpoC1</i>	0.0103	178.60
<i>rps15-ycf1</i>	0.0212	284.57
<i>trnE-trnT</i>	0.0241	522.51
<i>trnfM-psaB</i>	0.0254	375.76
<i>trnH-psbA</i>	0.0126	310.47
<i>trnK-rps16</i>	0.0164	350.44
<i>trnL</i>	0.0106	192.27
<i>trnT-psbD</i>	0.0239	291.15
<i>trnV-atpE</i>	0.0128	379.77
<i>ycf1</i> (1)	0.0273	462.53
<i>ycf1</i> (2)	0.0469	313.12

Note: π = nucleotide diversity; LD = differences in log-likelihood scores.

^aInformative windows identified in this study are indicated in bold.

^bHigh values (above the 95th percentile) for π and LD are indicated in bold.

the lack of conserved regions. Primers were designed to amplify across all 23 Neotropical species without the use of degenerate bases. However, primers with a small number of degenerate bases were permitted for some regions where primer development otherwise would not have been possible due to high sequence variability in the priming sites. We investigated the potential of our markers to produce robust phylogenies by calculating individual gene trees in RAxML version 8.2.9 in an ML search with 100 rapid bootstraps (option “-f a”) using the GTRGAMMA model. To evaluate the number of markers needed to obtain a resolved tree with an average of ~90 bootstrap support (BS), we first concatenated the two markers with the highest π and inferred a tree; subsequently, we added the marker with the next highest π score. We iterated this process until we obtained a matrix with each of the 10 markers developed. For every tree obtained, we calculated its average BS and its Robinson–Foulds distance (RF; Robinson and Foulds, 1981) from the plastome phylogeny using a custom

R script employing the packages APE (Paradis et al., 2004) and Phangorn (Schliep, 2011). The scripts and alignments used in this study can be found at https://bitbucket.org/oscarvargash/lecythidaceae_plastomes.

RESULTS

Lecythidaceae plastome features

The sequenced plastome of *B. excelsa* contained 160,472 bp and 115 genes, of which four were rRNAs and 30 were tRNAs (Fig. 1, Table 1). The arrangement of the *B. excelsa* plastome had a typical angiosperm quadripartite structure with a single-copy region of 85,830 bp, a small single-copy region of 16,670 bp, and two inverted repeat regions of 27,481 bp each. Relative to *C. sinensis* var. *pubilimba*, we found no gene gain/losses in *B. excelsa*. The only structural difference we found is that *B. excelsa* contains the sequential genes *trnH-GUG*, *rps3*, *rpl22*, and *rps19* in the inverted repeat region, whereas *C. sinensis* var. *pubilimba* contains these genes in the large single-copy region. Similarly, no gene gain/losses were found when *B. excelsa* was compared to other Neotropical Lecythidaceae plastomes assembled herein (Table 2). In addition to *B. excelsa*, the plastome of *Eschweilera alata* A. C. Sm. was also completely assembled; the coverage for the remaining plastomes ranged between 85% and 99.60% (Appendix 1).

Identification of molecular markers

Within the plastome of *B. excelsa* we found 23 cpSSRs, 22 of which were in non-coding regions and one in the *ndhD* coding region. We designed 19 primer pairs with an acceptable product length, annealing temperature, and GC content for cpSSRs located in non-coding regions (Table 3). π exceeded the 95th percentile for nine 600-bp windows (Fig. 2, Tables 4 and 5). Similarly, 13 windows were over the 95th percentile for LD (Fig. 2, Tables 4 and 5), indicating high phylogenetic signal. Although most of the informative windows were in non-coding regions, two consecutive regions were positioned in the *ycf1* gene. Six windows contained both high π and LD. As expected, high π and greater LD largely agreed. Based on the rank of the windows obtained for π , we developed primers for the following regions (ordered from high to low π): *ycf1*, *rpl16-rps3*, *psbM-trnD*, *ccsA-ndhD*, *trnG-psaB*, *petD-rpoA*, *psbZ-trnfM*, *trnE-trnT*, and *trnT-psbD* (Table 6).

TABLE 6. Primer sequences designed to amplify the 10 most polymorphic Lecythidaceae plastome regions, as sorted by decreasing nucleotide diversity.

Window in the alignment	π	Region	Forward primer sequence (5'–3')	Reverse primer sequence (5'–3')	Length (bp) ^a
144,103–145,487	0.04691	<i>ycf1</i> (1)	AGAACCTTTGATTATGTCTCGACG	AGAGACATGCTATAAAAATAGCCCA	1186
95,034–95,741	0.03446	<i>rpl16-rps3</i>	AGAGTTTCTTCTCATCCAGCTCC	GCTTAGTGTGTGACTCGTTGG	1014
35,585–36,413	0.02920	<i>psbM-trnD</i>	CCGTTCTTTCTTTTCTATAACCTACCC	ACGCTGGTCAAATCCAGCT	1093
143,235–144,102	0.02733	<i>ycf1</i> (2)	TGATTGCAATCTTTAGCATTAKAACT	KCGTCGAGACATAATCAAAGGT	1189
131,180–132,054	0.02576	<i>ccsA-ndhD</i>	CCGAGTGGTAAATAATGCACGT	GCTTCTTTCGATTACCGGG	1180
44,398–45,132	0.02537	<i>trnG-psaB</i>	TCGATYCCCGTATCCGCC	GCCAATTTGATTGATCGAGAGA	883
89,032–89,688	0.02464	<i>petD-rpoA</i>	TGGGAGTGTGTGACTTGAAC	TGACCCATCCCTTTAGCCAA	824
43,412–44,397	0.02456	<i>psbZ-trnfM</i>	TCCAATTGRCTGTTTTGCATTAATTG	CCTTGAGGTCACGGGTTCAA	706
37,444–38,345	0.02409	<i>trnE-trnT</i>	AGACGATGGGGGCATACCTG	CCACTACTTTTTCTTTTGTGTTGA	1324
38,346–40,085	0.02391	<i>trnT-psbD</i>	GGCGTAAGTCATCGGTTCAA	CCCAAAGCGAAATAGGCACA	1717

Note: π = nucleotide diversity.

^aThe product size (length) references the *Bertholletia excelsa* plastome.

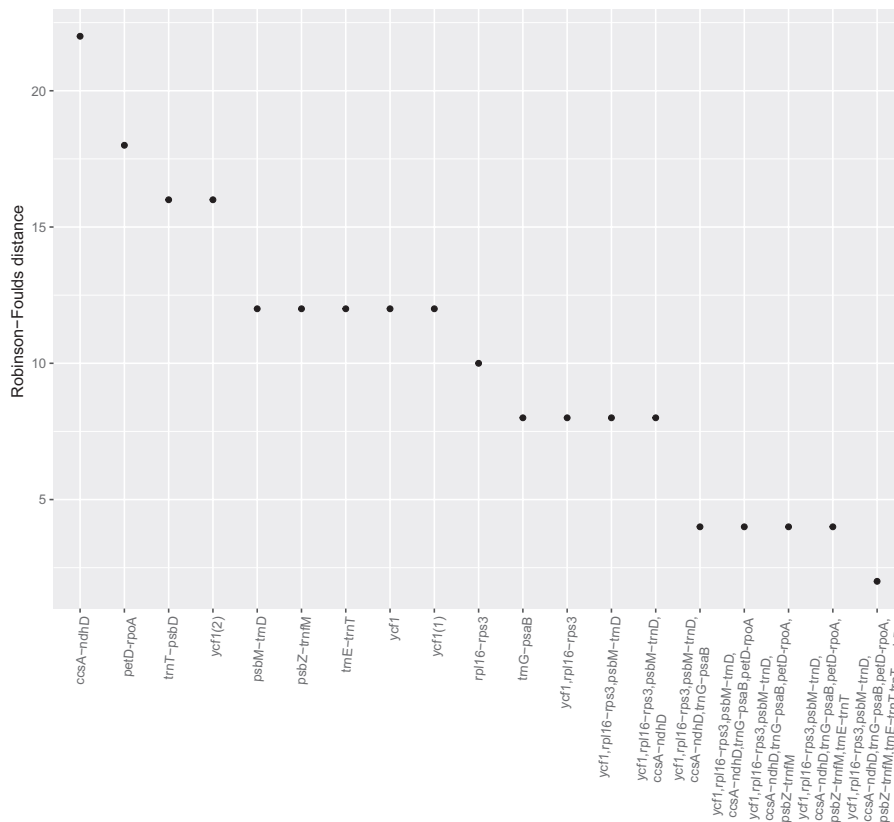


FIGURE 5. Robinson–Foulds distances (RF) for trees inferred from either independent or concatenated regions with high nucleotide diversity, sorted in descending order. Lower RF distances, which measure the number of different taxa bipartitions from the complete plastome topology, indicate better accuracy.

Walker et al. (2017). These calculations helped us to evaluate the performance of specific chloroplast regions as potential phylogenetic markers. The core plant DNA barcodes *matK* and *rbcL* did not exhibit high π or LD in our analysis (Table 5). Of the secondary plastome barcodes mentioned in the literature (*rpoC1*, *rpoB*, *trnL*, and *psbA-trnH*; Kress et al., 2005; Lahaye et al., 2008; Hollingsworth et al., 2009; Li et al., 2011), only *psbA-trnH* showed high LD (Table 5), although it did not exhibit exceptionally high values of π . In contrast, the regions *ycf1*, *rpl16-rps3*, *psbM-trnD*, *ccsA-ndhD*, *trnG-psaB*, *petD-rpoA*, *psbZ-trnM*, *trnE-trnT*, and *trnT-psbD* displayed the highest values of π and LD and therefore outperformed all of the previously proposed plant DNA barcodes.

Phylogenetic trees calculated from concatenated marker sets (based on the π rank) outperformed single regions in terms of support (BS) and accuracy (RF; Figs. 4, 5). In fact, tree topologies using single markers deviated from the complete plastome tree (mean RF = 13.8). The most well-performing concatenated matrix contained all 10 regions for which we developed primers. However, the combination of *ycf1* and *rpl16-rps3* produced an average BS of ~90 (Fig. 4) with reasonable accuracy (RF = 4, Fig. 5); we conclude that these two regions, amplified in three PCRs (Table 6), are promising markers for DNA barcoding, phylogeny, and phylogeography in Lecythidaceae. Although barcoding efficiency in species-rich clades (i.e., *Eschweilera/Lecythis*) might decline with the addition of more samples, *ycf1* and *rpl16-rps3* effectively distinguished between three closely related species within the *Eschweilera parvifolia* Mart. ex DC. clade (see branch

lengths in Appendix S1), suggesting that these markers might effectively distinguish between many other closely related species. Our results and conclusions agree with those of Dong et al. (2015), who proposed *ycf1* as a universal barcode for land plants.

The 19 cpSSR markers developed for non-coding portions of the *B. excelsa* plastome provide a useful resource for population genetic studies. Because of their fast stepwise mutation rate relative to single-nucleotide polymorphisms, cpSSRs can also be used for finer-grain phylogeographic analyses (e.g., Lemes et al., 2010; Twyford et al., 2013). This may be especially useful for species that exhibit little geographic structuring across parts of their ranges. Because they are maternally transmitted and can be variable within populations, the cpSSRs may also be used to track the dispersal of seeds and seedlings relative to the maternal source trees.

Because of their high level of polymorphism and phylogenetic signal content, we anticipate using the cpDNA markers presented here to study the phylogeography of widespread Lecythidaceae species such as *Couratari guianensis* Aubl. and *Eschweilera coriacea*, which range from the Amazon basin into Central America.

Barcoding of tropical trees

The DNA barcoding of tropical trees has been useful for several applications (Dick and Kress, 2009), including community phylogenetic analyses (Kress et al., 2009), inferring the species identity of the gut content (diet) of herbivores (García-Robledo et al., 2013), and for species identification of seedlings (Gonzalez et al., 2009). The power of DNA barcodes to discriminate among species should be high if the studied species are distantly related; for example, Kress et al. (2009) were able to discriminate 281 of 296 tree and shrub species from Barro Colorado Island using standard DNA barcodes, but they were not able to discriminate among some congeneric species in the species-rich genera *Inga* Mill. (Fabaceae), *Ficus* L. (Moraceae), and *Piper* L. (Piperaceae). Gonzalez et al. (2009) encountered similar challenges with *Eschweilera* species in their study of trees and seedlings in Paracou, French Guiana. The latter study tested a wide range of putative DNA barcode regions (*rbcLa*, *rpoC1*, *rpoB*, *matK*, *trnL*, *psbA-trnH*, and ITS) but did not include the markers presented in this article.

Limitations of plastome markers for phylogeny and species identification

These newly identified plastome markers are not free of limitations. First, plastome-based phylogenies should be interpreted with caution, as they can disagree with nuclear markers and species trees as a result of introgression and/or lineage-sorting issues (Rieseberg and Soltis, 1991; Sun et al., 2015; Vargas et al., 2017). These same processes limit the cpDNA for species identification. For example, cpDNA haplotypes of *Nothofagus* Blume, *Eucalyptus*

L'Hér., *Quercus* L., *Betula* L., and *Acer* L. were more strongly determined by geographic location than by species identity because of the occurrence of localized introgression within these groups (Petit et al., 1993; Palme et al., 2004; Saeki et al., 2011; Premoli et al., 2012; Nevill et al., 2014; Thomson et al., 2015). To date, the occurrence of haplotype sharing in closely related Lecythidaceae species has not been examined at a large scale and it is therefore not possible to conclude to what extent introgression or incomplete lineage sorting might affect this group. We suggest that future studies utilizing cpDNA barcodes for Neotropical Lecythidaceae test species from several shared geographic localities to examine to what extent haplotypes tend to be shared among species at the same localities. Nuclear DNA markers may also be used to examine phylogenetic incongruence and to identify cases where introgression might have occurred.

ACKNOWLEDGMENTS

The National Science Foundation (grant no. DEB 1240869 and FESD Type I 1338694 to C.W.D.) and the University of Michigan (Associate Professor Award to C.W.D.) provided financial support for this work. The authors thank Scott Mori, Gregory Stull, Caroline Parins-Fukuchi, Joseph Walker, and three anonymous reviewers for their useful comments, as well as Scott Mori and the New York Botanical Garden for providing access to curated DNA samples of Lecythidaceae.

DATA ACCESSIBILITY

DNA sequences have been deposited to GenBank (accession no. MF359935–MF359958 and BioProject SUB2740669). Plastome alignment, gene alignments, trees, and R code are available at https://bitbucket.org/oscarvargash/lecythidaceae_plastomes.

SUPPORTING INFORMATION

Additional Supporting Information (Appendix S1) may be found online in the supporting information tab for this article.

LITERATURE CITED

- Chambers, J. Q., N. Higuchi, and J. P. Schimel. 1998. Ancient trees in Amazonia. *Nature* 391: 135–136.
- Dexter, K. G., T. D. Pennington, and C. W. Cunningham. 2010. Using DNA to assess errors in tropical tree identifications: How often are ecologists wrong and when does it matter? *Ecological Monographs* 80: 267–286.
- Dick, C. W., and W. J. Kress. 2009. Dissecting tropical plant diversity with forest plots and a molecular toolkit. *BioScience* 59: 745–755.
- Dong, W., C. Xu, C. Li, J. Sun, Y. Zuo, S. Shi, T. Cheng, et al. 2015. *ycf1*, the most promising plastid DNA barcode of land plants. *Scientific Reports* 5: 8348.
- García-Robledo, C., D. L. Erickson, C. L. Staines, T. L. Erwin, and W. J. Kress. 2013. Tropical plant-herbivore networks: Reconstructing species interactions using DNA barcodes. *PLoS ONE* 8: e52967.
- Gonzalez, M. A., C. Baraloto, J. Engel, S. A. Mori, P. Pétronelli, B. Riéra, A. Roger, et al. 2009. Identification of Amazonian trees with DNA barcodes. *PLoS ONE* 4: e7483.
- Hollingsworth, P. M., L. L. Forrest, J. L. Spouge, M. Hajibabaei, S. Ratnasingham, M. van der Bank, M. W. Chase, et al. 2009. A DNA barcode for land plants. *Proceedings of the National Academy of Sciences, USA* 106: 12794–129797.
- Huang, Y. Y., S. A. Mori, and L. M. Kelly. 2015. Toward a phylogenetic-based generic classification of Neotropical Lecythidaceae—I. Status of *Bertholletia*, *Corythophora*, *Eschweilera* and *Lecythis*. *Phytotaxa* 203: 85–121.
- Katoh, K., K. Misawa, K. Kuma, and T. Miyata. 2002. MAFFT: A novel method for rapid multiple sequence alignment based on fast Fourier transform. *Nucleic Acids Research* 30: 3059–3066.
- Kearse, M., R. Moir, A. Wilson, S. Stones-Havas, M. Cheung, S. Sturrock, S. Buxton, et al. 2012. Geneious Basic: An integrated and extendable desktop software platform for the organization and analysis of sequence data. *Bioinformatics* 28: 1647–1649.
- Kress, W. J., K. J. Wurdack, E. A. Zimmer, L. A. Weigt, and D. H. Janzen. 2005. Use of DNA barcodes to identify flowering plants. *Proceedings of the National Academy of Sciences, USA* 102: 8369–8374.
- Kress, W. J., D. L. Erickson, F. A. Jones, N. G. Swenson, R. Perez, O. Sanjur, and E. Bermingham. 2009. Plant DNA barcodes and a community phylogeny of a tropical forest dynamics plot in Panama. *Proceedings of the National Academy of Sciences, USA* 106: 18621–18626.
- Lahaye, R., M. van der Bank, D. Bogarin, J. Warner, F. Pupulin, G. Gigot, O. Maurin, et al. 2008. DNA barcoding the floras of biodiversity hotspots. *Proceedings of the National Academy of Sciences, USA* 105: 2923–2928.
- Lemes, M. R., C. W. Dick, C. Navarro, A. J. Lowe, S. Cavers, and R. Gribel. 2010. Chloroplast DNA microsatellites reveal contrasting phylogeographic structure in mahogany (*Swietenia macrophylla* King, Meliaceae) from Amazonia and Central America. *Tropical Plant Biology* 3: 40–49.
- Li, D.-Z., L.-M. Gao, H.-T. Li, H. Wang, X.-J. Ge, J.-Q. Liu, Z.-D. Chen, et al. 2011. Comparative analysis of a large dataset indicates that internal transcribed spacer (ITS) should be incorporated into the core barcode for seed plants. *Proceedings of the National Academy of Sciences, USA* 108: 19641–19646.
- Librado, P., and J. Rozas. 2009. DnaSP v5: A software for comprehensive analysis of DNA polymorphism data. *Bioinformatics* 25: 1451–1452.
- Lohse, M., O. Drechsel, and R. Bock. 2007. OrganellarGenomeDRAW (OGDRAW): A tool for the easy generation of high-quality custom graphical maps of plastid and mitochondrial genomes. *Current Genetics* 52: 267–274.
- Martin, M. 2011. Cutadapt removes adapter sequences from high-throughput sequencing reads. *EMBnet.journal* 17: 10–12.
- Mayer, C. 2010. Phobos. Website http://www.rub.de/spezzoo/cm/cm_phobos.htm [accessed 1 February 2017].
- Mori, S. A. 2017. The Lecythidaceae pages. Website <http://sweetgum.nybg.org/science/projects/lp/> [accessed 1 February 2017].
- Mori, S. A., and G. T. Prance. 1987. A guide to collecting Lecythidaceae. *Annals of the Missouri Botanical Garden* 74: 321–330.
- Mori, S. A., and G. T. Prance. 1990. Lecythidaceae. Part II. The zygomorphic-flowered New World genera (*Couroupita*, *Corythophora*, *Bertholletia*, *Couratari*, *Eschweilera*, & *Lecythis*). In K. Kubitzki and S. Renner [eds.], *Flora Neotropica Monographs*, vol. 21, part 2. New York Botanical Garden, Bronx, New York, USA.
- Mori, S. A., C. H. Tsou, C. C. Wu, B. Cronholm, and A. A. Anderberg. 2007. Evolution of Lecythidaceae with an emphasis on the circumscription of Neotropical genera: Information from combined *ndhF* and *trnL-F* sequence data. *American Journal of Botany* 94: 289–301.
- Mori, S. A., E. A. Kiernan, N. P. Smith, L. M. Kelley, Y.-Y. Huang, G. T. Prance, and B. Thiers. 2017. Observations on the phylogeography of the Lecythidaceae clade (Brazil nut family). *Phytoneuron* 30: 1–85.
- Nei, M. 1987. *Molecular evolutionary genetics*. Columbia University Press, New York, New York, USA.
- Nevill, P. G., T. Després, M. J. Bayly, G. Bossinger, and P. K. Ades. 2014. Shared phylogeographic patterns and widespread chloroplast haplotype sharing in *Eucalyptus* species with different ecological tolerances. *Tree Genetics and Genomes* 10: 1079–1092.
- Palme, A. E., Q. Su, S. Palsson, and M. Lascoux. 2004. Extensive sharing of chloroplast haplotypes among European birches indicates hybridization among *Betula pendula*, *B. pubescens* and *B. nana*. *Molecular Ecology* 13: 167–178.

- Paradis, E., J. Claude, and K. Strimmer. 2004. APE: Analyses of phylogenetics and evolution in R language. *Bioinformatics* 20: 289–290.
- Petit, R. J., A. Kremer, and D. B. Wagner. 1993. Geographic structure of chloroplast DNA polymorphisms in European oaks. *Theoretical and Applied Genetics: International Journal of Plant Breeding Research* 87: 122–128.
- Prance, G. T., and S. A. Mori. 1979. Lecythidaceae—Part I. The actinomorphic-flowered New World Lecythidaceae (*Asteranthos*, *Gustavia*, *Grias*, *Allantoma*, & *Cariniana*). In K. Kubitzki and S. Renner [eds.], *Flora Neotropica Monographs*, vol. 21, part 1. New York Botanical Garden, Bronx, New York, USA.
- Premoli, A. C., P. Mathiasen, M. C. Acosta, and V. A. Ramos. 2012. Phylogeographically concordant chloroplast DNA divergence in sympatric *Nothofagus* s.s. How deep can it be? *New Phytologist* 193: 261–275.
- R Core Team. 2017. R: A language and environment for statistical computing. R Foundation for Statistical Computing, Vienna, Austria. Website <https://www.r-project.org/> [accessed 1 March 2017].
- Rieseberg, L. H., and D. E. Soltis. 1991. Phylogenetic consequences of cytoplasmic gene flow in plants. *Evolutionary Trends in Plants* 5: 64–84.
- Robinson, D. F., and L. R. Foulds. 1981. Comparison of phylogenetic trees. *Mathematical Biosciences* 53: 131–147.
- Sablok, G., G. V. Padma Raju, S. B. Mudunuri, R. Prabha, D. P. Singh, V. Baev, G. Yahubyan, et al. 2015. ChloroMitoSSRDB 2.00: More genomes, more repeats, unifying SSRs search patterns and on-the-fly repeat detection. *Database* 2015: 1–10.
- Saeki, I., C. W. Dick, B. V. Barnes, and N. Murakami. 2011. Comparative phylogeography of red maple (*Acer rubrum* L.) and silver maple (*Acer saccharinum* L.): Impacts of habitat specialization, hybridization and glacial history. *Journal of Biogeography* 38: 992–1005.
- Schliep, K. P. 2011. phangorn: Phylogenetic analysis in R. *Bioinformatics* 27: 592–593.
- Schmieder, R., and R. Edwards. 2011. Quality control and preprocessing of metagenomic datasets. *Bioinformatics* 27: 863–864.
- Stamatakis, A. 2014. RAxML version 8: A tool for phylogenetic analysis and post-analysis of large phylogenies. *Bioinformatics* 30: 1312–1313.
- Sukumaran, J., and M. T. Holder. 2010. DendroPy: A Python library for phylogenetic computing. *Bioinformatics* 26: 1569–1571.
- Sun, M., D. E. Soltis, P. S. Soltis, X. Zhu, J. G. Burleigh, and Z. Chen. 2015. Deep phylogenetic incongruence in the angiosperm Rosidae clade. *Molecular Phylogenetics and Evolution* 83: 156–166.
- ter Steege, H., N. C. A. Pitman, D. Sabatier, C. Baraloto, R. P. Salomão, J. E. Guevara, O. L. Phillips, et al. 2013. Hyperdominance in the Amazonian tree flora. *Science* 342: 325–342.
- Thomson, A. M., C. W. Dick, and S. Dayanandan. 2015. A similar phylogeographical structure among sympatric North American birches (*Betula*) is better explained by introgression than by shared biogeographical history. *Journal of Biogeography* 42: 339–350.
- Twyford, A. D., C. A. Kidner, N. Harrison, and R. A. Ennos. 2013. Population history and seed dispersal in widespread Central American *Begonia* species (Begoniaceae) inferred from plastome-derived microsatellite markers. *Botanical Journal of the Linnean Society* 171: 260–276.
- Untergasser, A., I. Cutcutache, T. Koressaar, J. Ye, B. C. Faircloth, M. Remm, and S. G. Rozen. 2012. Primer3: New capabilities and interfaces. *Nucleic Acids Research* 40: e115.
- Vargas, O. M., E. M. Ortiz, and B. B. Simpson. 2017. Conflicting phylogenomic signals reveal a pattern of reticulate evolution in a recent high-Andean diversification (Asteraceae: Astereae: *Diplostephium*). *New Phytologist* 214: 1736–1750.
- Walker, J. F., J. W. Brown, and S. A. Smith. 2017. Analyzing contentious relationships and outlier genes in phylogenomics. *bioRxiv*. <https://doi.org/10.1101/115774>
- Wyman, S. K., R. K. Jansen, and J. L. Boore. 2004. Automatic annotation of organellar genomes with DOGMA. *Bioinformatics* 20: 3252–3255.
- Zerbino, D. R., and E. Birney. 2008. Velvet: Algorithms for de novo short read assembly using de Bruijn graphs. *Genome Research* 18: 821–829.

APPENDIX 1. Lecythidaceae species sequenced with their voucher, assembly information, and GenBank accession number. All voucher specimens are deposited at the New York Botanical Garden Herbarium (Bronx, New York, USA).

Species	Voucher	No. of reads	% of ref seq ^a	Mean coverage	No. of contigs	Average length of assembled contigs (bp)	Minimum contig length (bp)	Maximum contig length (bp)	N50	GenBank accession no.
<i>Allantoma decandra</i> (Ducke) S. A. Mori, Ya Y. Huang & Prance	Mori 25640	527,449	99.20	213	9	157,957	1052	42,447	22,733	MF359949
<i>A. lineata</i> (Mart. & O. Berg) Miers	Chevalier 10101	697,746	99.60	295	8	158,449	400	34,633	32,463	MF359941
<i>Barringtonia edulis</i> Seem.	Tsou 1552	519,377	96.10	230	10	152,805	2636	46,991	32,608	MF359956
<i>Bertholletia excelsa</i> Bonpl.	Mori 25637	1,036,874	100	646	14	160,472	461	160,472	160,472	MF359948
<i>Cariniana estrellensis</i> (Raddi) Kuntze	Nee 52828	759,042	85	292	70	130,037	278	22,237	3803	MF359938
<i>Corythophora amapaensis</i> Pires ex S. A. Mori & Prance	Mori 24148	690,545	99.60	302	4	159,222	6643	75,002	42,750	MF359955
<i>C. labriculata</i> (Eyma) S. A. Mori & Prance	Mori 25518	606,728	99.60	260	5	158,819	6596	74,896	42,691	MF359946
<i>Couratari macrosperma</i> A. C. Sm.	Janovec 2506	340,696	99	144	9	156,981	1107	45,975	42,740	MF359944
<i>C. stellata</i> A. C. Sm.	Mori 24093	493,777	99.40	211	6	158,312	1374	109,344	109,344	MF359936
<i>Couroupita guianensis</i> Aubl.	Mori 25516	503,417	96.50	314	12	154,792	1071	47,693	18,977	MF359935
<i>Eschweilera alata</i> A. C. Sm.	Prévost 4607	851,683	100	358	2	158,981	61,051	97,930	97,929	MF359940
<i>E. caudiculata</i> R. Knuth	Cornejo 8185	273,053	98.30	116	11	156,630	1117	37,154	21,598	MF359957
<i>E. integrifolia</i> (Ruiz & Pav. ex Miers) R. Knuth	Cornejo 8211	440,144	99	187	9	157,206	1105	42,497	21,591	MF359942
<i>E. micrantha</i> (O. Berg) Miers	Mori 25410	289,775	98.90	120	11	157,890	1143	42,551	18,021	MF359958
<i>E. pittieri</i> R. Knuth	Cornejo 8208	160,625	97	166	8	154,547	551	74,876	24,636	MF359954

(Continues)

APPENDIX 1. (continued)

Species	Voucher	No. of reads	% of ref seq ^a	Mean coverage	No. of contigs	Average length of assembled contigs (bp)	Minimum contig length (bp)	Maximum contig length (bp)	N50	GenBank accession no.
<i>E. wachenheimii</i> (Benoist) Sandwith	Prévost 4252	367,631	98.90	151	11	157,757	1179	37,141	21,748	MF359939
<i>Grias cauliflora</i> L.	Aguilar 7961	520,480	94.90	326	41	150,768	314	28,189	8102	MF359952
<i>Gustavia augusta</i> L.	Mori 24255	761,640	95.50	476	33	152,601	358	28,353	11,657	MF359943
<i>G. serrata</i> S. A. Mori	Cornejo 8184	534,143	98.90	334	10	157,746	1035	35,586	22,762	MF359947
<i>Lecythis ampla</i> Miers	Cornejo 8229	606,518	94.10	241	39	149,464	348	28,759	6527	MF359951
<i>L. congestiflora</i> Benoist	Molino 2019	1,073,567	96.90	405	27	154,882	302	21,264	11,580	MF359937
<i>L. corrugata</i> Poit.	Mori 24265	544,831	90.70	243	50	143,859	317	28,741	4496	MF359950
<i>L. minor</i> Jacq.	Tsou 1542	666,355	94.80	416	26	151,568	354	31,188	14,768	MF359945
<i>L. pneumatophora</i> S. A. Mori	Mori 25728	690,202	99.50	301	4	158,832	11,782	75,019	49,184	MF359953

^aPercentage of the sequence recovered in relation to *Bertholletia excelsa*.